Autonomous DNA nanomachine based on cascade amplification of strand displacement and DNA walker for detection of multiple DNAs

Kun Wang, Meng-Qi He, Fu-Heng Zhai, Jin Wang, Rong-Huan He, Yong-Liang Yu

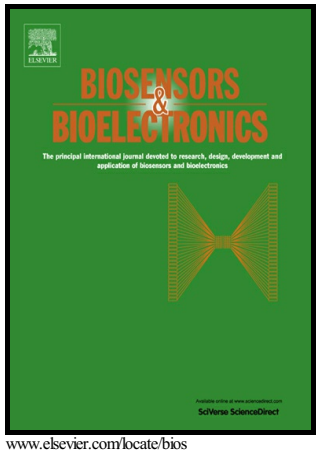

www.elsevier.com/locate/bios

PII: S0956-5663(18)30056-3
DOI: https://doi.org/10.1016/j.bios.2018.01.044
Reference: BIOS10237

To appear in: *Biosensors and Bioelectronic*

Received date: 28 October 2017
Revised date: 18 January 2018
Accepted date: 19 January 2018

Cite this article as: Kun Wang, Meng-Qi He, Fu-Heng Zhai, Jin Wang, Rong-Huan He and Yong-Liang Yu, Autonomous DNA nanomachine based on cascade amplification of strand displacement and DNA walker for detection of multiple DNAs, *Biosensors and Bioelectronic,* https://doi.org/10.1016/j.bios.2018.01.044

Autonomous DNA nanomachine based on cascade amplification of strand displacement and DNA walker for detection of multiple DNAs

Kun Wang, Meng-Qi He, Fu-Heng Zhai, Jin Wang, Rong-Huan He*, Yong-Liang Yu*

Department of Chemistry, College of Sciences, Northeastern University, Box 332, Shenyang 110819, China

Corresponding Authors

*E-mail: herh@mail.neu.edu.cn (R.-H. He)

*E-mail: yuyl@mail.neu.edu.cn (Y.-L. Yu)

Tel: +86 24 83688944; Fax: +86 24 83676698

ABSTRACT: DNA can be modified to function as a scaffold for the construction of a DNA nanomachine, which can then be used in analytical applications if the DNA nanomachine can be triggered by the presence of a diagnostic DNA or some other analyte. We herein propose a novel and powerful DNA nanomachine that can detect DNA via combining the tandem strand displacement reactions and a DNA walker. Three different DNA sensing platforms are described, where the whole DNA machine was constructed on a gold electrode (GE). This cascade multiple amplification strategy exhibited an excellent sensitivity. Under optimal conditions, the electrochemical sensor could achieve a detection limit of 36 fM with a linear range from 50 to 500 fM. In particular, the electrochemical sensor could easily distinguish the base mutations. More interestingly, the DNA nanomachine could be used to construct analog AND and OR logic gates. We demonstrate that electrochemical signals generated from the different input combinations can be used to distinguish multiple target DNAs. The practical applicability of the present biosensor is demonstrated by the detection of target DNA in human serum with satisfactory results, which holds great potential for a future application in clinical diagnosis.

Graphical Abstract

A versatile, and intelligent DNA nanomachine is constructed for multiple DNA detection with high sensitivity and selectivity.

Keywords: DNA walker, cascade amplification, biosensor, intelligent detection

1. Introduction

Substantial efforts have been made to improve the sensitivity of DNA detection, and numerous amplification platforms have been developed, including polymerase chain reaction (Kumar et al. 2002; Shu et al. 2017), enzyme assisted cycling (Zhang et al. 2015b; Zhou et al. 2014), nanomaterials (Lin et al. 2017; Wang et al. 2018), and signal amplification based on artificial DNA machines (Li et al. 2016b; Lv et al. 2015). Among these approaches, DNA machines have attracted widespread attention due to their structural simplicity, ease of construction, sufficient sequence design space, and predictable molecular behavior (Yin et al. 2008; Zhang and Seelig 2011; Zhang et al. 2014). Taking advantage of their versatility, specificity, and predictability of DNA hybridization, various DNA machines have been constructed, including DNA tweezers (Liu et al. 2013; Yurke et al. 2000), DNA motors (Cha et al. 2014; Liber et al. 2015), DNA robots (Amir et al. 2014; Lund et al. 2010), and DNA walkers (He et al. 2017; Li et al. 2017b; Qu et al. 2017). In particular, DNA walkers can run autonomously on their designated tracks and have great application potential in biological sensing (Peng et al. 2017; Zhang et al. 2015a). Recently, DNA tracks have been built on nanomaterials, including gold films (Yehl et al. 2016), nanoparticles (Jung et al. 2016), and nanotubes (Cha et al. 2015), making use of the mobility and processivity of the DNA walkers (Li et al. 2017a; Liang et al. 2017).

The cascade amplification strategy is another important strategy for amplified detection of DNA (Gu et al. 2017; Wang et al. 2015). In order to obtain a high sensitivity, a series of cascade DNA circuits have been proposed through the integration of DNA machines, including catalytic hairpin assemblies (Yin et al. 2008), hybridization chain reactions (Tang et al. 2012; Venkataraman et al. 2007), rolling circle amplification (Cheglakov et al. 2007; Wang et al. 2014; Zeng et al. 2013),

enzyme-assisted amplification (Orbach et al. 2012; Wang et al. 2017; Xu et al. 2016; Xu et al. 2015), and DNA walker (Wang et al. 2015). Dong's group reported a cascade amplification strategy based on a combination of different nucleases (Wang et al. 2017). Bi's group developed a circuit by integrating a catalytic hairpin assembly with the hybridization chain reaction (Bi et al. 2016). Wang's group proposed an amplification strategy on the basis of the integration of a DNA walker with rolling circle amplification for the detection of miRNAs (Wang et al. 2015). Despite the development of these strategies, they have encountered some disadvantages. First, enzyme-assisted amplification is limited by the reaction conditions (Li et al. 2016a). Second, the hairpin self-assembly not only leads to a high background (Jiang et al. 2013), but also increases the experimental time (Jiang et al. 2014). Therefore, there is still an urgent need to develop a DNA amplification strategy, which is nuclease-free, simple, and has a high signal-to-noise ratio.

We present here a systematic research of the cascade system to improve the amplified detection of DNA using a combination of strand displacement and a metal-ion dependent DNAzyme-derived DNA walker. The DNA nanomachine integrated strand displacement and DNA walker avoids the employment of nuclease and hairpin self-assembly, giving rise to a high signal-to-noise ratio and high sensitivity. In this strategy, the target DNA triggers a series of strand displacement reactions to release the DNA walker (a Pb^{2+}-dependent DNAzyme). Subsequently, the DNA walker can walk on the surface of the gold electrode (GE) by cleaving the substrate-DNA, which then produces high signal intensity. The proposed electrochemical aptasensor exhibits an excellent performance for detection of the target DNA with a detection limit of 36 fM. The practical applicability of the present biosensor is demonstrated by the detection of target DNA in human serum with satisfactory results. Moreover, the DNA nanomachine is available to be used as analog AND and OR logic gates. We

demonstrate that the signal output, based on different input combinations, can be used to distinguish multiple target DNAs through utilization of combinatorial logic gates (AND and OR). Recently, we have developed an amplification strategy for the detection of CEA, which is activated by a conformational change in an aptamer (He et al., 2017). This hairpin-free and nuclease-free amplification strategy has a high signal-noise ratio, and is therefore potential for application in disease diagnosis and therapy.

2. Experimental section

2.1. Chemicals and Materials

DNA oligonucleotides were synthesized by Shanghai Sangon Biotechnology Co (Shanghai, China). The quality inspection reports of corresponding oligonucleotides were sent along with the products to prove the successful preparation of oligonucleotides. DNA oligonucleotide solutions were prepared by dissolving the DNAs in 25 mM Tris-HCl buffer containing 200 mM NaCl (pH 7.4), and quantified by using UV–visible absorption spectroscopy (Varian, USA) and measuring the absorbance at 260 nm. Table S1 shows the sequences of the oligonucleotides used in the study. All other chemicals were purchased from Aladdin (Shanghai, China), and used as received without further purification. Milli-Q ultrapure water (18.2 MΩ cm) was used through the experiments.

2.2. Surface Modification of the Electrode

The gold electrode (GE) with a diameter of 3 mm was initially polished first with 0.3 μm and followed with 0.05 μm alumina slurry until a mirror plane was formed. The GE was sonicated in a mixture of ethanol and ultrapure water for 1 min to remove excess Al_2O_3 powder. Then the GE was electrochemically cleaned in a 0.1 M H_2SO_4 solution with successive cyclic voltammetry (CV) scans from -0.2 V to 1.5 V until

reproducible voltammograms were observed. The GE was finally washed with ultrapure water and dried with nitrogen.

A mixture of the DNAzyme strand ((6), 2 μM), help strand ((7), 2 μM), and block strand ((8), 2 μM) in 25 mM Tris-HCl buffer (200 mM NaCl, pH 7.4) was heated at 90°C for 10 min, and then allowed to cool down to room temperature for at least 1 h to form the three-stranded DNA duplex. 2.5 μL of three-stranded DNA duplex (2 μM), 50μL of substrate strand (2 μM) and 10 μL of Tris(2-carboxyethyl)phosphine (TCEP, 10 mM) were added into Tris-HCl buffer to a total volume of 100 μL to obtain a mixture of 0.05 μM three-stranded DNA duplex and 1 μM substrate strand. After incubation for 1 h to reduce the disulfide bonds, 10 μL of the above mixture was dropped on GE and further incubated at 4°C for 12 h. After rinsing with phosphate buffer solution (PBS) and drying with nitrogen, the modified GE was incubated with 1mM freshly prepared 6-mercapto-1-hexanol (MCH) for 10 min to reduce nonspecific adsorption.

2.3. Cascade Amplification Strategy

The modified GE was incubated in 200 μL of 25 mM Tris-HCl buffer containing the fuel strand ((9), 0.1 μM) along with various concentrations of target DNA at room temperature. After incubation for 1 h, the electrode was washed by 25 mM Tris-HNO_3 buffer (pH 7.4) with 200 mM $NaNO_3$, 5 mM KNO_3, 1 mM $Mg(NO_3)_2$. Then, Pb^{2+} (1000 μM) was added to initiate the DNA walker. The electrode was afterwards washed with buffer and dried with nitrogen, respectively, before the electrochemical measurement to remove any remaining physi-sorbed methylene blue or Pb^{2+} (Fig. S11). Electrochemical measurements were conducted by using the CHI660C electrochemistry workstation (Co. Chenhua, China) with a platinum electrode as the auxiliary electrode, an Ag/AgCl electrode as the reference electrode, and the modified GE as the working electrode. Square wave voltammetry (SWV) was carried out in 20

mL of 25 mM Tris-HCl buffer with a potential window ranging from -0.4 V to -0.1 V, a step potential of 4 mV, and an amplitude of 25 mV. Electrochemical impedance spectroscopy (EIS) was performed by using a 5 mM $Fe(CN)_6^{3-/4-}$ solution containing 0.1 M KCl.

2.4. Native Polyacrylamide Gel Electrophoresis

Polyacrylamide gels (12%) were prepared with 1 × Tris-borate-EDTA buffer (89mM Tris, 89mM boric acid, 2mM EDTA, pH 8.3). The samples for gel electrophoresis were prepared by adding different components in solution and reacted for 1 h. Each sample was prepared in a 1 × Tris-borate-EDTA buffer containing 12 mM Mg^{2+}, and the concentration of each DNA strand was 2 μM. 20 μL of each sample was mixed with 2 μL of Gel-Dye Super Buffer Mix before loading into the gel. The gel was run under a constant voltage of 100 V over a period of ca. 2.5 h. Photographs were taken under UV light by using a fluorescence imaging system (Life Science Research Products and System Engineering, China).

3. Results and discussion

3.1. Detection Principle of DNA walker

The free-running DNA walker presented here was constructed on a functionalized GE onto which hundreds of substrate DNAs (3) and dozens of swing arm DNAs (2) were attached. The swing arm DNA (2) was composed of a poly-thymine spacer and a DNAzyme. The DNAzyme was blocked by using a locking DNA (1). For detection purposes, we labelled the substrate DNAs (3) with methylene blue (MB). When the DNA walker was inactive, the MB in the substrate DNAs (3) generated a high electrochemical signal (Fig. 1). Once the target DNA (T1-DNA) was present, the T1-DNA hybridized with the locking DNA (1) by a strand-displacement reaction, releasing the Pb^{2+}-dependent DNAzyme. The unlocked DNAzyme

hybridized to the substrate DNA (3) and cleaved the substrate DNA (3), releasing the MB-labelled fragment (4) and making the DNAzyme available for hybridization with another the substrate DNA (3). Thus, enzymatic cleavage provided the energy for autonomous walking of the DNAzyme on the GE. Each walking step was accompanied by the cleavage of the substrate DNA (3) and the release of the MB-labelled fragment (4). As the MB becomes detached from the GE, the electrochemical signal decreased significantly (Fig. 1). Monitoring the electrochemical signal enabled real-time detection of the motion of the DNA walker and the T1-DNA.

We first characterized the surface of the GE by using electrochemical impedance spectroscopy (EIS). As shown in Fig. S1A, the bare GE had a low electron transfer resistance. The resistance increased significantly after conjugation of strands (1,2) and (3), due to the formation of a DNA layer on the GE. After incubation of the GE with T1-DNA and Pb^{2+}, a dramatic decrease in electrochemical impedance was observed, indicating that the unlocked DNAzyme could cleave the substrate DNAs (3) to dissociate the MB-labelled fragments (4) from the surface of the GE. In addition to electrochemical impedance spectroscopy (EIS), we have also used cyclic voltammetry (CV) to characterize the surface. $[Fe(CN)_6]^{3-/4-}$ was used as an efficient indicator for electrode surface characteristics. As shown in Fig. S1B, a pair of symmetrical redox peaks was observed by using unmodified GE (black curve). When GE was modified with (3) and (1,2), the peak-to-peak potential difference increased obviously and the peak current decreased in the meantime, indicating that the electron transfer was restrained and strands (3) and (1,2) were successfully immobilized on GE. Upon the addition of T1-DNA and Pb^{2+}, the potential difference decreased and peak current increased, indicating the successful cleavage of substrate on GE. The variations of potential difference and peak current showed a reasonable trend in line with the estimate. To confirm the cleavage of the substrate DNAs (3), polyacrylamide gel

electrophoresis (PAGE) analysis was made to assess the state of the DNA components after the reaction was allowed to occur. As shown in Fig. S1C, the bands in lanes 1, 2, 3, 4, 5, and 6 correspond to strands (1), (2), (3), the T1-DNA, a duplex of (1)/T1-DNA, and (1)/(2), respectively. In the absence of T1-DNA, the cleavage reaction could not be triggered (lane 7), because the DNAzyme was blocked by (1). When T1-DNA was present, two new bands (in lane 8) indicated the products of the DNAzyme (2), and a duplex of (1)/T1-DNA. The disappearance of the band representing (3) suggested successful cleavage of the substrate DNAs (3). These data directly demonstrated the feasibility of the DNA walker. As shown in Fig. S1D, no current change (curve a) is observed on the DNA walker sensor in the absence of the T1-DNA, because of the blocked DNAzyme. The incubation of the sensor with either the T1-DNA (curve b) or Pb^{2+} (curve c) alone causes negligible current changes. It is because that the DNA walker cannot be initiated in the absence of the T1-DNA or Pb^{2+}. When both T1-DNA and Pb^{2+} are incubated with the sensor, a significant change in the current response (curve d) is observed. Current changes are mainly due to the release of DNAzyme, which cleaves the substrate strand on the surface of electrode as shown in Fig. 1. The results shown here clearly demonstrate the great potential of our approach for sensitive detection of DNA.

3.2. Feasibility and Optimizations

The key concept of the DNA walker in our work is the high mobility of the DNA walker after initiation. For this purpose, the length of the strands (2) and (3), and the Pb^{2+} concentration all play major roles in the performance of the reaction. We first optimized the length of the (2)/(3) duplex. (3) was composed of two domains; the fragment at the 3'-end of (2) was a 5-thymine spacer that was conjugated to the GE, which enhanced the accessibility of the S-DNA and the DNAzyme. The fragment (4) labelled with MB at the end of 5' was the binding region for the DNAzyme. The

DNAzyme consisted of a catalytic core flanked by two binding domains (the green domains of (3)). As shown in Fig. 1, once the DNA walker was initiated, the DNAzyme hybridized to (3) through the two binding domains. Hence, longer binding domains can significantly enhance the binding efficiency between the (2) and (3), thereby enhancing the cleavage events. However, a too long binding domain may reduce the mobility of the DNA walker, while an excess length of DNA duplex will impede the DNAzyme hybridizing with another (3), affecting the reaction rate (Fig. S2). Therefore, we chose the (2)/(3) duplex with 11 base pairs. The poly-thymine spacer served as the swing arm of DNA walker. We compared the performances of our nanomachine with different lengths of swing arm (poly-thymine spacer) for (2) to make sure the swing arm was long enough to provide sufficient DNAzyme to cleave most (3) on the GE. The progress curves from the operation of the nanomachine (Fig. S3) indicate that (2) provided sufficient DNAzyme to cleave most (3) on the GE when the swing arm was 60 nucleotides in length. As metal cofactors are a critical component of the DNAzyme, the operation of the DNA walker was tested at different concentrations of Pb^{2+}. As seen in Fig. S4A, the performance of DNA walker was significantly enhanced by increasing the concentration of the metal cofactor up to 1000 μM. It was then leveled off within 1000-2000 μM. The stability of this DNA nanomachine was investigated by monitoring five independent experiments at the same experimental conditions. As shown in Fig. S4B, it can be concluded that the reproducibility of the DNA nanomachine was acceptable.

3.3. Analytical Performance of the DNA-walker Biosensor

Under the optimized operating conditions for the DNA walker, we used the DNA nanomachine to determine different concentrations of target DNA (T1-DNA). As expected, the electrochemical signal gradually decreased with the increase in concentrations of T1-DNA, which is consistent with the fact that the higher

concentration of T1-DNA, the more activated DNA walker molecules. As shown in Fig. 2A, a higher concentration of T1-DNA led to larger current decreases. These time curves suggest that the DNA walker operates in three distinct phases. In the first phase, the DNAzyme cleaved the substrate at an original linear rate for ca. 15 min. DNAzyme hybridization positions the walker in close proximity to the substrate, and the subsequent cleavage followed steady state kinetics. When a large amounts of substrates were cleaved, there were few remaining substrate molecules available for the DNAzyme to act upon. The DNA walker operation therefore entered a slower phase (15-20 min). Finally, the operation of the DNA walker was completed when no substrate remains accessible (20-60 min). The current (I) is defined as the corresponding peak current of the square wave voltammetry (SWV) curve exposed to the solution of T1-DNA at various concentrations. As shown in Fig. 2B, the change in current increased with increasing concentrations of T1-DNA. The peak current decreased with increasing concentrations of T1-DNA (Fig. 2C). A linear relationship between peak current and concentrations of T1-DNA was obtained within the range from 10 to 100 pM (Fig. 2D). The equation for this linear relationship was determined to be $I=0.0268\times C_T(pM)-4.318$ ($R = 0.996$), where C_T is the concentration of T1-DNA. The detection limit was estimated to be 6.2 pM at a signal-to-noise ratio of 3. We hypothesized that there was a lower detection limit, because the confinement of (2) and (3) on the GE surface led to a high local concentration of DNAzyme and its substrate. To prove it, we compared the detection performance of the DNA walker with that of the free control DNAzyme. This analytical platform has important advances compared to the free-DNAzyme approach shown in Fig. S5. The detection limit for the free-DNAzyme approach is 171 pM, which is significantly higher than that of DNA walker approach (Fig. S6). The LOD of the DNA walker is about 27-fold lower than that of free-DNAzyme approach.

3.4. Detection Principle of Cascade Amplification Strategy

Further improvement of the sensor platform was achieved by combining strand displacement with the DNA walker, and the route was shown in Fig. 3. The cascade amplification strategy consisted of two components, i.e., the strand displacement reaction (SDR) and the DNA walker system. The strand displacement cycle was constructed by using four oligonucleotides ((6), (7), (8), (9)). The nucleotide (6), (7) and (8) hybridized to form a complex (6)/(7)/(8). In the absence of T1-DNA, (6) was hybridized with (7) and (8). The DNA walker system was assembled on the GE, and the DNAzyme (6) was silenced by the (6)/(7)/(8) complex. Once T1-DNA was added, it first bound to the toehold domain on the block-strand (8) to form a four-stranded structure (S1). The help-strand (7) spontaneously dissociated from S1, because the binding between (7) and (8) was too weak to keep (7) attached. The S1 was then transformed to the intermediate (S2) through branch migration. The red domain of (8) was then exposed, and this facilitates the binding of the fuel-strand (9) to form S3, which was then quickly rearranged by branch migration to release (6), T1-DNA and duplex (8)/(9). The regenerated T1-DNA then initiated a new recycling process, leading to the association of abundant single-strands (6) with the GE. The nucleotide (6) was designed to be a Pb^{2+}-assisted DNAzyme, which can cleave (3) and release a MB-labelled fragment (4). The principle of the DNA walker is the same as the one shown in Fig. 1. The unlocked (6) then hybridized to (3) on the GE, forming the DNAzyme/substrate complex (6)/(3). The DNAzyme subsequently cleaved (3) at its cleavage site with the assistance of Pb^{2+}. After being cleaved by the DNAzyme, (3) was split into two short pieces and thus resulted in a decrease of the electrochemical signal. Meanwhile, the leaving nucleotide (6) with a free recognition arm bound to an adjacent (3) by a strand displacement reaction, which ensured that the (6) continuously walked on the surface of GE and cleaved (3) in the process. Hence,

considerable signal amplification was gained. In brief, the automatic amplification mechanism we designed was composed of two cascade cycles. First, a small amount of T1-DNA initiated a series of SDRs, leading to release a large amount of (6) containing the Pb^{2+}-assisted DNAzyme. Second, the DNAzyme catalyzed substrate cleavage, and then moved from one substrate to the next. This self-powered DNA walker therefore achieved autonomous, free, and processive walking on the GE. Each walking step resulted in the cleavage of (3) and the release of the MB-labelled DNA strand (4) from GE. Thus, each walking step of the DNA walker resulted in a decrease in the electrochemical signal. This isothermal amplification mechanism is therefore expected to achieve a high sensitivity for the detection of T1-DNA, because of the integration of the SDR with the DNA walker.

3.5. Analytical Performance of Cascade Amplification Strategy

Under the new optimized operating conditions (Fig. S7), the electrochemical response in the presence of different amounts of T1-DNA was evaluated. T1-DNA triggered the SDR to yield abundant DNA walker strands (6), which could walk on the surface of GE as described above. When (6) walked on the GE, different amounts of (3) were cleaved, which significantly changed the electrochemical signal. The peak current gradually decreased with increasing T1-DNA concentrations as shown in Fig. 4A. The peak current was also proportional to the T1-DNA concentration (Fig. 4B). There was a linear relationship between peak current and concentrations of T1-DNA within the range from 50 to 500 fM. The equation for this linear relationship was determined to be $I=0.00317\times C_T(fM)-4.113$ ($R = 0.995$). In addition, the detection limit was estimated to be 36 fM at a signal-to-noise ratio of 3, indicating high sensitivity with respect to previously developed approaches (Table S2). This remarkable sensitivity was achieved through two aspects of the design. First, multiple

turnover of the T1-DNA becomes a significant factor in increasing sensitivity. Second, (6) can cleave the abundant (3) to obtain the signal response.

In addition to sensitivity, a high specificity is especially important in diagnosis and therapy. Thus, the specificity of the proposed sensing system was investigated in the presence of various mutants of T1-DNA. Here, mutants containing a single-base mismatch (M1a and M1b), which is the most frequently occurring genetic variation, were analyzed by using the present sensing system. As shown in Fig. 4C, T1-DNA can cause significant signal change, while the M1a and M1b mutants resulted in signal changes of 20.9% and 26.3% with respect to that caused by T1-DNA, respectively. An even smaller signal change was observed in the presence of DNA containing two-base mismatches (M2a and M2b), and a three-base mismatch (M3). The results validate the excellent selectivity of the assay for the detection of T1-DNA.

To explore the feasibility of the developed strategy in biological medium, the sensing platform was also employed to detect the T1-DNA in human serum samples. The human serum samples were diluted with reaction buffer 100 times prior to detection. Then, the T1-DNA was detected in these human blood plasma samples following the same procedure. As shown in Fig. 4D, obvious electrochemical signal changes were found for target DNA detection in both buffer solution and serum. The results indicated the potential applicability of the proposed method for DNA detection in real biological samples. As far as disease diagnosis is concerned, it needs to develop a sensor with an ultralow detection limit and outstanding selectivity. Hence, the cascade amplification strategy holds great potential for future application in clinical diagnosis.

3.6. Construction of Combinatorial Logic Operation of AND and OR Gates

The developed assay can be used to construct logic circuits. First, the DNA nanomachine was used to construct an analog AND gate, where both the target DNAs

are required to initiate the nanomachine. A simplified schematic of the AND gate is shown in Fig. 5A. In the presence of any one target DNA T1-DNA or T2-DNA, each could initiate its own SDR, respectively. However, there was no significant signal change, due to the absence of free-DNAzyme. When T1-DNA and T2-DNA were present together, the DNAzyme was released because of the two SDRs. The free-DNAzyme was able to walk on the surface of GE, and a large number of substrate strands were cleaved, which dramatically decreased the electrochemical signal. Herein, T1-DNA, T2-DNA, and the peak current change are defined as input 1, input 2, and output, respectively. In Fig. 5B, the absence or presence of T1-DNA/T2-DNA is defined as "0" or "1", respectively. The output signal is defined as "0" or "1" when the peak current is bigger than -2 μA or smaller than -2 μA, respectively. The corresponding truth table is shown in Fig. 5C. As expected, the logic circuit fits the characteristics of an AND logic gate.

The AND logic gate is a potential sensor for the detection of multiple analytes. However, it cannot distinguish between two inputs, which is one of the inherent disadvantages of the AND logic gate. To further promote the application of our detection strategy in intelligent analyte detection, we designed a combinatorial logic gate (OR and AND) for intelligently judging which targets were present in a sample. The principle of the OR logic gate is shown in Fig. S8A. In brief, the P1-DNA could directly displace the block DNA and release the DNAzyme. The DNAzyme then cleaved the MB-functionalized substrate (3) to yield the MB-labelled strand (4), resulting in the electrochemical signal change. When neither T1-DNA nor P1-DNA was present, there was big electrochemical signal due to a blocked DNA nanomachine. However, upon addition of T1-DNA or P1-DNA, a significant signal decrease was observed due to initiation of the DNA nanomachine. In the presence of both T1-DNA and P1-DNA, the electrochemical signal resulting from T1-DNA and P1-DNA has the

smallest electrochemical signal (Fig. S8B). We define the absence or presence of T1-DNA/P1-DNA as “0” or “1”, respectively. Meanwhile, the output signal is defined as “0” or “1” when the peak current is bigger than -2 μA or smaller than -2 μA, respectively. The truth table corresponding to the OR logic gate is shown in Fig. S8C. Subsequently, another OR logic gate for T2-DNA was designed in similar way as the previous OR logic gate by using T2-DNA and P2-DNA as inputs. As shown in Fig. S9A, the electrochemical signal was clearly changed after the addition of T2-DNA or P2-DNA, or the complex of T2-DNA/P2-DNA. It is because that the release of the DNAzyme and cleavage of the MB-functionalized substrate induce a change in the electrochemical signal (Fig. S9B). These data were also in accord with the truth table for the OR logic gate (Fig. S9C).

For the purpose of intelligent detection, a combinatorial logic gate (OR and AND) was constructed to assess if the targets were present in a sample (Fig. 6A). The definition of inputs and outputs are the same as previously described. On the basis of the outputs, the ingredients in a sample can be logically deduced. As shown in Fig. 6B, we inputted samples to the DNA nanomachine under the same conditions for the AND logic gate. If a significant signal change was observed, we could conclude that both T1-DNA and T2-DNA were present in the sample, and no further analysis was required. It is because that only in this case the signal change could be obtained according to the AND logic. If sample was added to the system and there was no signal change, the solution cannot contain both T1-DNA and T2-DNA. However, it would be impossible to know the composition of the sample. In such a situation, we could reach a conclusion with the help of the OR logic gate. Firstly, the P1-DNA and sample were added to the system together. The input P1-DNA can release the 5’ of DNAzyme according to the OR logic. If the signal changed, the other end of DNAzyme must be released by the SDR initiated by T2-DNA. It would indicate that

the sample contained T2-DNA but not T1-DNA. On the other hand, if the mixture of P1-DNA and sample resulted in no signal changes, there are only two cases: only T1-DNA was present in the sample or no target DNA (i.e., neither T1-DNA nor T2-DNA). In this situation, P2-DNA and sample should be added together. If a big signal change was observed, we could be sure that only T1-DNA was present in the sample and T2-DNA was absent. In the case that a signal change could only be obtained by adding P1-DNA, P2-DNA and the sample together, there was no target DNA (i.e., neither T1-DNA nor T2-DNA). It was because that the DNA nanomachine could be started if P1-DNA and P2-DNA were present together. The corresponding SWV curve is shown in Fig. S10. Based on the aforementioned analysis, we demonstrate that the cascade amplification reaction is powerful to intelligently detect multiple DNAs. Hence, this cascade amplification strategy might be useful in the intelligent detection of biomolecules as well as cancer cells.

4. Conclusions

In summary, we have developed an electrochemical detection protocol for the quantitative detection of a target DNA by coupling the SDR with a DNA walker machine. The addition of target DNA triggers the SDR to generate a massive amount of DNAzyme for the DNA walker machine. When the DNAzyme walks on the surface of the GE, a large number of substrate strands are cleaved, leading to a significant electrochemical signal change. The present strategy allows the sensitive detection of target DNA down to 36 fM. This autonomous cascade amplification strategy abandons the cumbersome and expensive thermal cycling protocol, making it easily applicable for clinical diagnosis. Moreover, the combinatorial logic operation integrated by the AND and OR logic gates provides a new approach for multiplex target recognition. Finally, the amplification strategy reported here can distinguish

single-base mismatched mutants from the target DNA, with a high specificity. It is reasonable to expect that the cascade amplification strategy has a significant potential application in point-of-care clinical diagnosis.

Acknowledgments

This work is financially supported the Natural Science Foundation of China (51572044, 21475018), and the Fundamental Research Fund for the Central Universities (N160504010).

References

Amir, Y., Ben-Ishay, E., Levner, D., Ittah, S., Abu-Horowitz, A., Bachelet, I., 2014. Nat. Nanotechnol. 9, 353-357.

Bi, S., Yue, S., Wu, Q., Ye, J., 2016. Chem. Commun. 52, 5455-5458.

Cha, T.-G., Pan, J., Chen, H., Robinson, H.N., Li, X., Mao, C., Choi, J.H., 2015. J. Am. Chem. Soc. 137, 9429-9437.

Cha, T.-G., Pan, J., Chen, H., Salgado, J., Li, X., Mao, C., Choi, J.H., 2014. Nat. Nanotechnol. 9, 39-43.

Cheglakov, Z., Weizmann, Y., Basnar, B., Willner, I., 2007. Org. Biomol. Chem. 5, 223-225.

Gu, Y., Song, J., Li, M.-X., Zhang, T.-T., Zhao, W., Xu, J.-J., Liu, M., Chen, H.-Y., 2017. Anal. Chem. 89, 10585-10591.

He, M. Q., Wang, K., Wang, W. J., Yu, Y. L., Wang, J. H., 2017. Anal. Chem. 89, 9292-9298.

Jiang, Y., Li, B., Milligan, J.N., Bhadra, S., Ellington, A.D., 2013. J. Am. Chem. Soc.135, 7430-7433.

Jiang, Y.S., Bhadra, S., Li, B., Ellington, A.D., 2014. Angew. Chem.-Int. Edit. 53, 1845-1848.

Jung, C., Allen, P.B., Ellington, A.D., 2016. Nat. Nanotechnol. 11, 157-163.

Kumar, R., Vandegraaff, N., Mundy, L., Burrell, C.J., Li, P., 2002. J. Virol. Methods 105, 233-246.

Li, N., Zheng, J., Li, C., Wang, X., Ji, X., He, Z., 2017a. Chem. Commun. 53, 8486-8488.

Li, W., Wang, L., Jiang, W., 2017b. Chem. Commun. 53, 5527-5530.

Li, X., Peng, Y., Chai, Y., Yuan, R., Xiang, Y., 2016a. Chem. Commun. 52, 3673-3676.

Li, X., Ye, S., Luo, X., 2016b. Chem. Commun. 52, 10269-10272.

Liang, C.-P., Ma, P.-Q., Liu, H., Guo, X.-G., Ye, B.-C., 2017, Angew. Chem.-Int. Edit. 56, 9077-9081.

Liber, M., Tomov, T.E., Tsukanov, R., Berger, Y., Nir, E., 2015. Small 11, 568-575.

Lin, X., Liu, Y., Tao, Z., Gao, J., Deng, J., Yin, J., Wang, S., 2017. Biosens. Bioelectron. 94, 471-477.

Liu, M., Fu, J., Hejesen, C., Yang, Y., Woodbury, N.W., Gothelf, K., Liu, Y., Yan, H., 2013. Nat. Commun. 4, e2127.

Lund, K., Manzo, A.J., Dabby, N., Michelotti, N., Johnson-Buck, A., Nangreave, J., Taylor, S., Pei, R., Stojanovic, M.N., Walter, N.G., Winfree, E., Yan, H., 2010. Nature 465, 206-210.

Lv, Y., Cui, L., Peng, R., Zhao, Z., Qiu, L., Chen, H., Jin, C., Zhang, X.-B., Tan, W., 2015. Anal. Chem. 87, 11714-11720.

Orbach, R., Mostinski, L., Wang, F., Willner, I., 2012. Chem.-Eur. J. 18, 14689-14694.

Peng, H., Li, X.-F., Zhang, H., Le, X.C., 2017. Nat. Commun. 8, e14378.

Qu, X., Zhu, D., Yao, G., Su, S., Chao, J., Liu, H., Zuo, X., Wang, L., Shi, J., Wang, L., Huang, W., Pei, H., Fan, C., 2017. Angew. Chem.-Int. Edit. 56, 1855-1858.

Shu, B., Zhang, C., Xing, D., 2017. Biosens. Bioelectron. 97, 360-368.

Tang, W., Wang, D., Xu, Y., Li, N., Liu, F., 2012. Chem. Commun. 48, 6678-6680.

Venkataraman, S., Dirks, R.M., Rothemund, P.W.K., Winfree, E., Pierce, N.A., 2007. Nat. Nanotechnol. 2, 490-494.

Wang, D., Xiao, X., Xu, S., Liu, Y., Li, Y., 2018. Biosens. Bioelectron. 99, 431-437.

Wang, F., Lu, C.-H., Liu, X., Freage, L., Willner, I., 2014. Anal. Chem. 86, 1614-1621.

Wang, K., Fan, D., Liu, Y., Dong, S., 2017. Biosens. Bioelectron. 87, 116-121.

Wang, L., Deng, R., Li, J., 2015. Chem. Sci. 6, 6777-6782.

Xu, J., Wu, Z.-S., Li, H., Wang, Z., Le, J., Zheng, T., Jia, L., 2016. Biosens. Bioelectron. 86, 1024-1030.

Xu, J., Wu, Z.-S., Shen, W., Xu, H., Li, H., Jia, L., 2015. Biosens. Bioelectron. 73, 19-25.

Yehl, K., Mugler, A., Vivek, S., Liu, Y., Zhang, Y., Fan, M., Weeks, E.R., Salaita, K., 2016. Nat. Nanotechnol. 11, 184-190.

Yin, P., Choi, H.M.T., Calvert, C.R., Pierce, N.A., 2008. Nature 451, 318-322.

Yurke, B., Turberfield, A.J., Mills, A.P., Simmel, F.C., Neumann, J.L., 2000. Nature 406, 605-608.

Zeng, Y.P., Hu, J., Long, Y., Zhang, C.Y., 2013. Anal. Chem. 85, 6143-6150.

Zhang, D.Y., Seelig, G., 2011. Nat. Chem. 3, 103-113.

Zhang, F., Nangreave, J., Liu, Y., Yan, H., 2014. J. Am. Chem. Soc. 136, 11198-11211.

Zhang, H., Lai, M., Zuehlke, A., Peng, H., Li, X.F., Le, X.C., 2015. Angew. Chem.-Int. Edit. 54, 14326-14330.

Zhang, H., Li, M., Li, C., Guo, Z., Dong, H., Wu, P., Cai, C., 2015b. Biosens. Bioelectron. 74, 98-103.

Zhou, W., Gong, X., Xiang, Y., Yuan, R., Chai, Y., 2014. Biosens. Bioelectron. 55, 220-224.

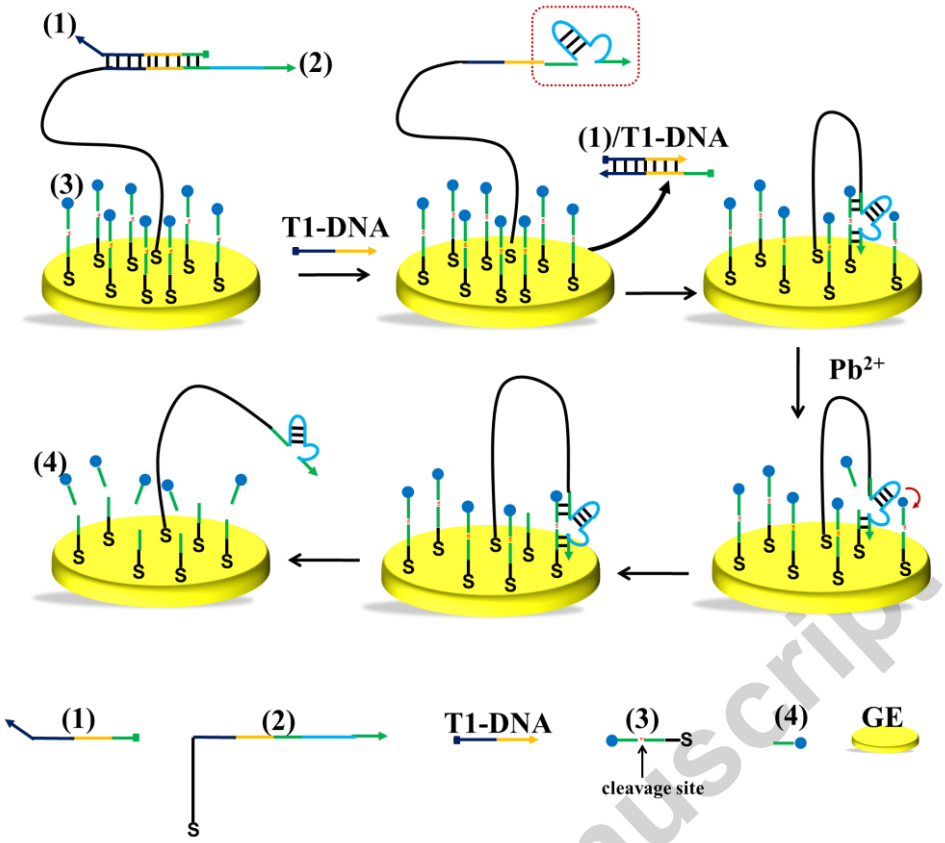

Fig. 1. Amplified analysis of a target DNA through a Pb^{2+}-dependent DNAzyme-derived DNA walker.

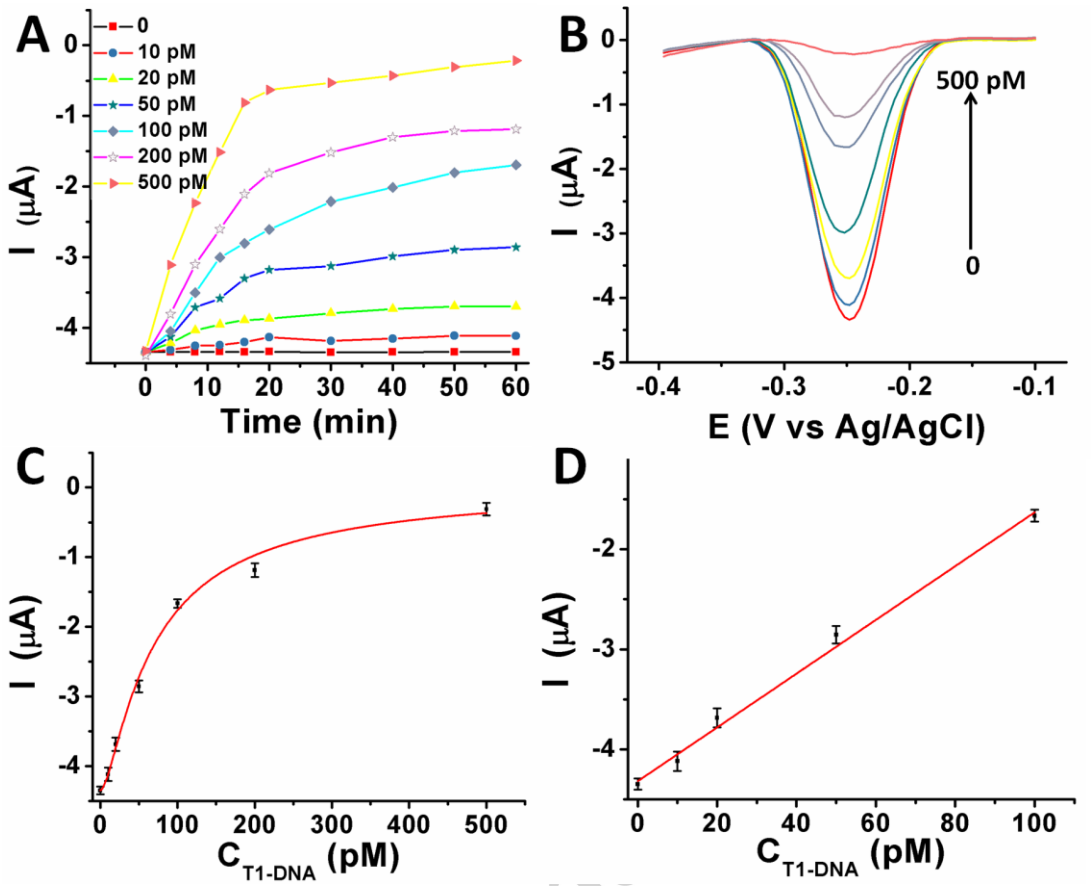

Fig. 2. (A) Time dependent current changes at different T1-DNA concentrations according to the scheme outlined in Fig. 1; (B) SWV responses corresponding to the analysis of different concentrations of T1-DNA ranging from 0 to 500 pM at a fixed time-interval of 1 h; (C) The peak current in the presence of various concentrations of T1-DNA; (D) Calibration curve of peak current versus T1-DNA concentration.

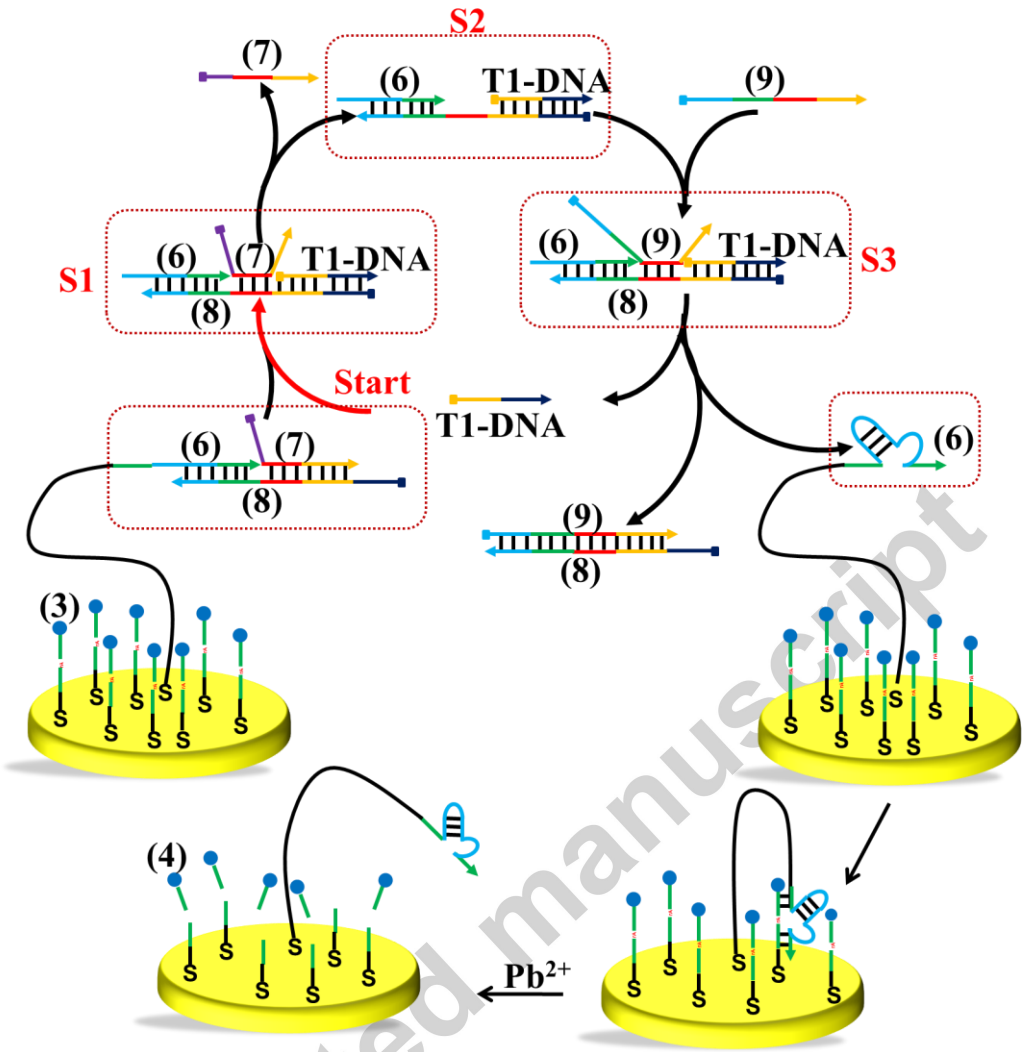

Fig. 3. Amplified analysis of a target DNA through a cascade isothermal amplification reaction.

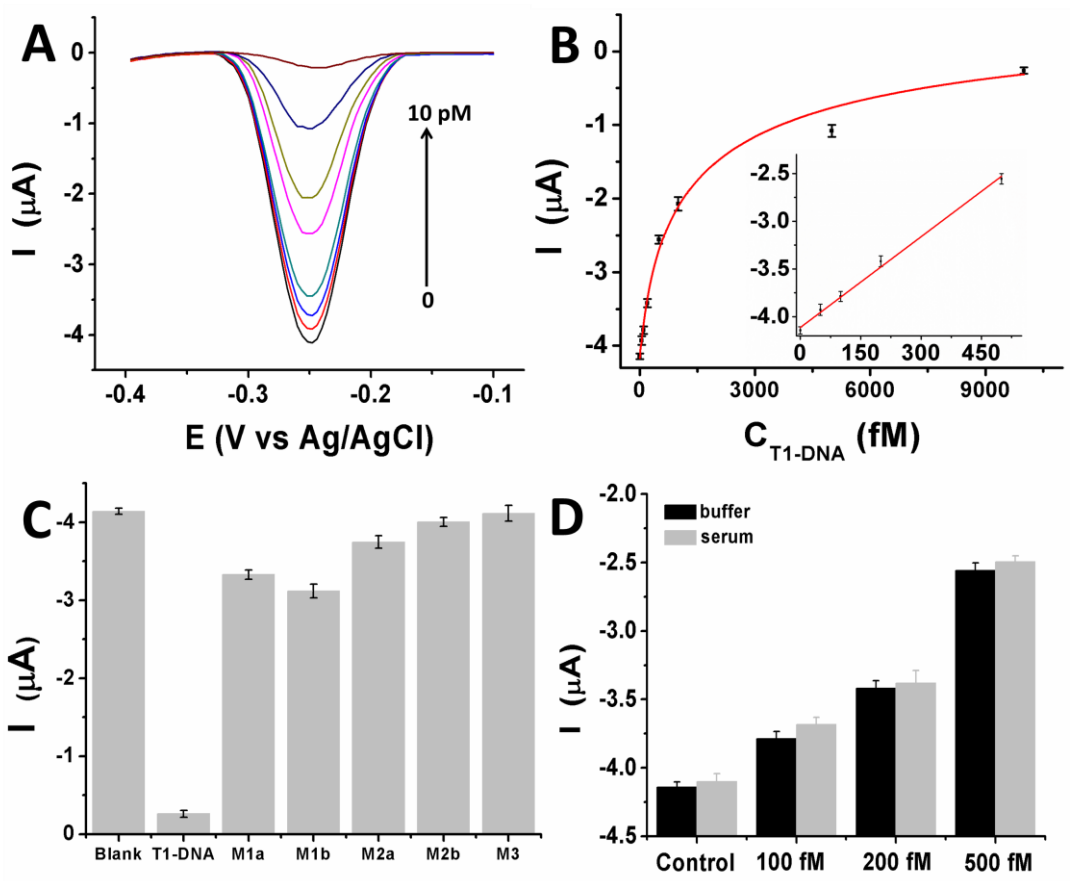

Fig. 4. (A) SWV responses corresponding to the analysis of different concentrations of T1-DNA ranging from 0 to 10 pM according to the scheme outlined in Fig. 3; (B) The peak current in the presence of various concentrations of T1-DNA. Inset: calibration curve of peak current versus T1-DNA concentration; (C) The peak current in the presence of T1-DNA (10 pM), and mutants (10 pM): M1a, M1b, M2a, M2b, M3; (D) Results obtained from the electrochemical tests of buffer solution and the diluted serum samples spiked with different concentrations of T1-DNA. The same reaction mixtures without T1-DNA were used as controls. The reaction conditions were the same as the cascade amplification strategy.

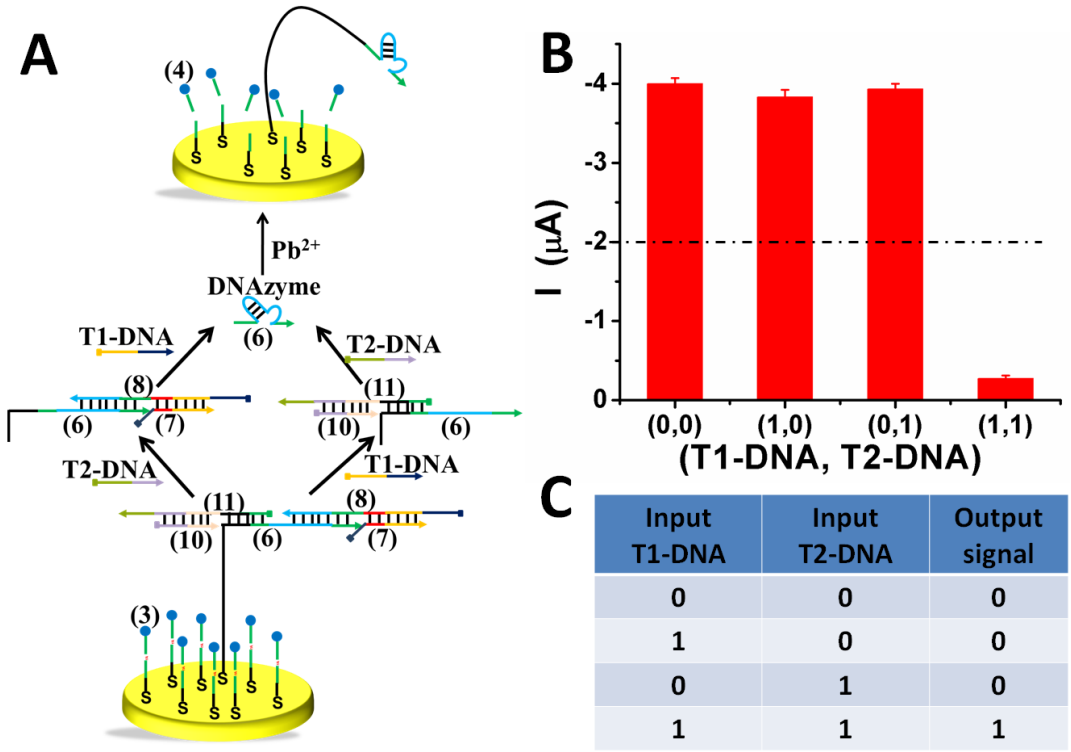

C

Input T1-DNA	Input T2-DNA	Output signal
0	0	0
1	0	0
0	1	0
1	1	1

Fig. 5. (A) Schematic of the AND logic gate function; (B) Column values of the peak current output; (C) Truth table for the AND logic gate. The reaction conditions were the same as the cascade amplification strategy, and the SWV response was collected after incubation for 1 h.

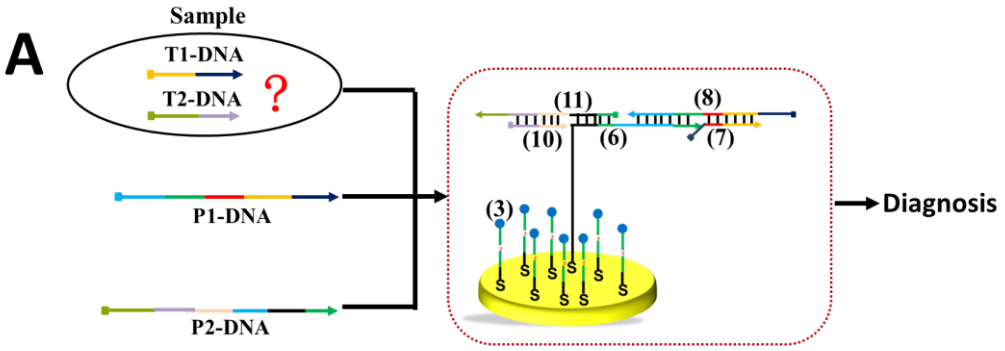

B

Input						Diagnosis
	Sample	1	1	1	1	
	P1-DNA	0	1	0	1	
	P2-DNA	0	0	1	1	
Output		1	\	\	\	Contain T1-DNA and T2-DNA
		0	1	\	\	Contain T2-DNA
		0	0	1	\	Contain T1-DNA
		0	0	0	1	No target

Fig. 6. (A) Schematic of the combinatorial logic gates for the intelligent detection of T1-DNA and T2-DNA in samples; (B) Truth table for the combinatorial logic gates. The "\" symbol means that the corresponding condition can be omitted. The reaction conditions were the same as the cascade amplification strategy, and the SWV response was collected after incubation for 1 h.

Graphical Abstract

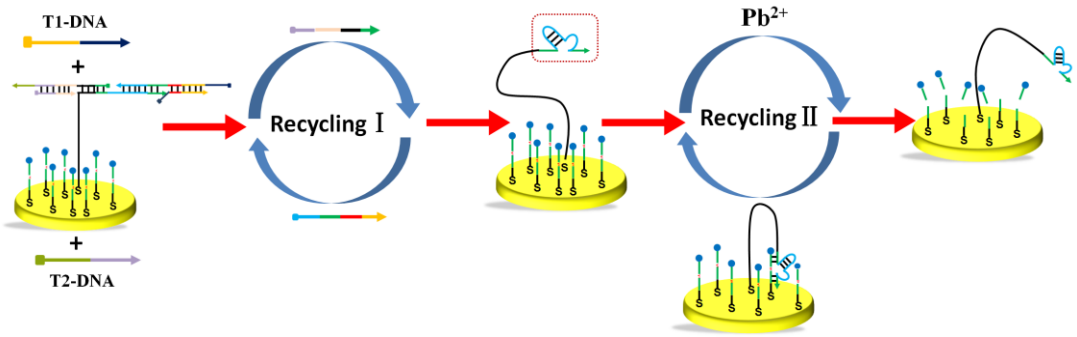

Highlights:

- An autonomous DNA nanomachine is developed for detection of multiple DNAs.
- The proposed cascade amplification strategy achieves a detection limit of 36 fM for target DNA.
- Single-base mismatched mutant from target DNA can be distinguished by the present assay.
- Multiple DNAs can be individually detected under a combinatorial logic gate control.